



**SUPERCONDUCTING COIL TRAINING AND INSTABILITIES
DUE TO THE BAUSCHINGER EFFECT**

J. R. Heim

June 13, 1974

ABSTRACT

For many years the marginal performance of many superconducting coils has been tolerated because of a lack of understanding as to the cause of the observed effects. Study efforts and laboratory experiments have identified electrical losses associated with coil performance but unidentified mechanical losses which generate heat and degrade coil performance have been overlooked. This manuscript describes the inelastic behavior of superconducting composite conductors which must be considered if coil performance is to be reasonably evaluated. The experimental techniques used and the results obtained are described. The significance of the results is assessed and methods of eliminating mechanical losses are described. A new process for stabilizing the superconductor matrix metal, the PWP process (post wind preload) is presented.



INTRODUCTION

Most superconducting coils operate in a liquid helium environment at temperatures near 4°K. Since the current carrying capability of the superconductor is strongly dependent upon the superconductor temperature much effort has been devoted to maintaining the superconductor temperature as close as possible to the helium bath temperature. These methods include:

- (1) helium flow channels built into the coil structure to allow the coolant to come into direct contact with the conductor
- (2) high conductivity metallic fins (heat drains) sandwiched between layers of wire to conduct the generated heat into the helium bath
- (3) loaded epoxies to conduct heat through the coil structure and into the helium bath

The first of these methods (flow channels) has been used extensively in the past with good results but inherent with this type of construction one is satisfied with lower current densities in the coil and the resultant coil volume is large. For many applications coil volume is not a constraint and the above construction is adequate. However, for many other applications small coil volume is of great importance and the latter 2 methods of construction are used. The last method of construction (potted coils) approaches the ideal coil in that the finished product is rugged and

capable of carrying high current densities, but the methods of analysis must be refined to accommodate a less conservative design.

Let us interpret the last sentence in straight forward engineering language. If we sacrifice cooling capability for higher current densities we must identify and understand all sources of heat or the stability calculations will not accurately predict coil performance. Temperature - specific heat and temperature - enthalpy curves show the heat content of conductor materials to be very small at liquid helium temperatures with the heat content approaching zero as temperature decreases. Therefore, small sources of heat may not be neglected. i.e. seemingly small sources of heat may produce a significant temperature rise and coil stability is dominated by conductor temperature. All heat sources must be accounted for if coil stability is to be guaranteed.

One of the major heat sources which has been overlooked is a mechanical loss due to inelastic behavior of the matrix metal used to stabilize the superconductor. The following discussion identifies these losses and describes their effect on coil stability.

ANALYTICAL APPROACH

The following work started out as a simple effort to explore the limits of a coil type construction which has been used successfully to build large superconducting magnets for high energy physics experiments. To refine the methods of analysis used to design these coils the first step was to

-3-

determine the prestressed condition of the coil conductor just prior to charging for the first time. Simplifying assumptions had been made in the past and the validity of these assumptions has been investigated with significant results.

A representative superconducting wire specimen was chosen for analysis and subsequent testing. Specimen wire data is shown below.

Material - niobium titanium (N_bTi)
with a copper matrix

wire diameter - .040 inches

copper to superconductor ratio - 4/1

filament diameter - .002 inches

number filaments - 84

twist pitch - 2 per inch

The character of the partners making up the composite was then considered. Copper is a good superconductor stabilizing metal in the softened condition but a poor structural material. Niobium titanium on the other hand is radically different. N_bTi is a tough metal with a very high elastic strain capability. Also, the expansion coefficients of the two metals differ by more than a factor of two. In line with the above considerations, simplifying assumptions as to the residual stress condition of the composite components after the manufacturing process is not justified.

Manufacturing Process Effects

1 - drawing

Looking back into the wire manufacturing processes one can choose a stage where the stress condition of both components is known fairly well. The obvious choice is the final draw immediately following twisting. This final draw is performed to "set the twist". An initial assumption then followed:

AT FINAL DRAW BOTH METALS EXIT THE DRAWING DIE STRESSED TO THEIR ULTIMATE STRENGTHS AS SHOWN

$N_b T_i$	175,000 p.s.i.
Cu	45,000 p.s.i. (true stress)

2 - annealing

The next manufacturing process is a heat treatment to soften the copper. This anneal process is considered "company proprietary information" by most manufacturers but similarity of processes justifies assumptions. The following heat treatment assumptions were made:

- (1) THE COPPER IS SOFTENED TO THE FULL ANNEAL CONDITION
- (2) THE WIRE IS WOUND TIGHTLY ON A STEEL SPOOL FOR HEAT TREATMENT

Using the above assumptions we may now proceed to calculate the internal stress condition of the wire. First, we assume that the $N_b T_i$ is uniformly distributed throughout the

-5-

copper. Second, we neglect the effects of twisting (twisting effects will be considered later). The internal stress is best described by the average strain differential ($\delta\epsilon$) between the $N_b T_i$ and copper as

$$(1) \quad \delta\epsilon = \epsilon_s - \epsilon_c = \left(\frac{\sigma}{E}\right)_s - \left(\frac{\sigma}{E}\right)_c$$

where $\delta\epsilon$ = differential strain

ϵ = component strain

σ = component stress

E = component modulus of elasticity

subscripts designate superconductor (S) and copper (C)

positive strain corresponds to tensile stress

negative strain corresponds to compressive stress

We obtain a second equation from equilibrium. The longitudinal force in the copper must be equal and opposite to the longitudinal force in the $N_b T_i$

$$F_s + F_c = A_s \sigma_s + A_c \sigma_c = 0$$

solving for σ_s

$$(2) \quad \sigma_s = \frac{-A_c}{A_s} \sigma_c$$

where A_c/A_s is the copper superconductor ratio

Substituting equation (2) into equation (1) and solving for σ_c

$$(3) \quad \sigma_c = \frac{\delta\epsilon}{\frac{A_c}{A_s E_s} + \frac{1}{E_c}}$$

-6-

Thermal strains due to a difference in length change of the components with respect to temperature change are treated in a similar manner.

$$(4) \quad \delta\epsilon_T = \epsilon_S - \epsilon_C = \left[\frac{L_{RT} - L_T}{L_{RT}} \right]_S - \left[\frac{L_{RT} - L_T}{L_{RT}} \right]_C$$

where $\delta\epsilon_T$ = differential thermal strain

L_T = component length at temperature

L_{RT} = component length at room temperature

Using equations (1) through (4) and a stress-strain curve for annealed copper the residual stresses in the wire components has been calculated for room temperature and liquid helium temperature. The results of these calculations for copper to superconductor ratios from 1 to 20 are shown in figure 1. These data show that the residual stresses remaining

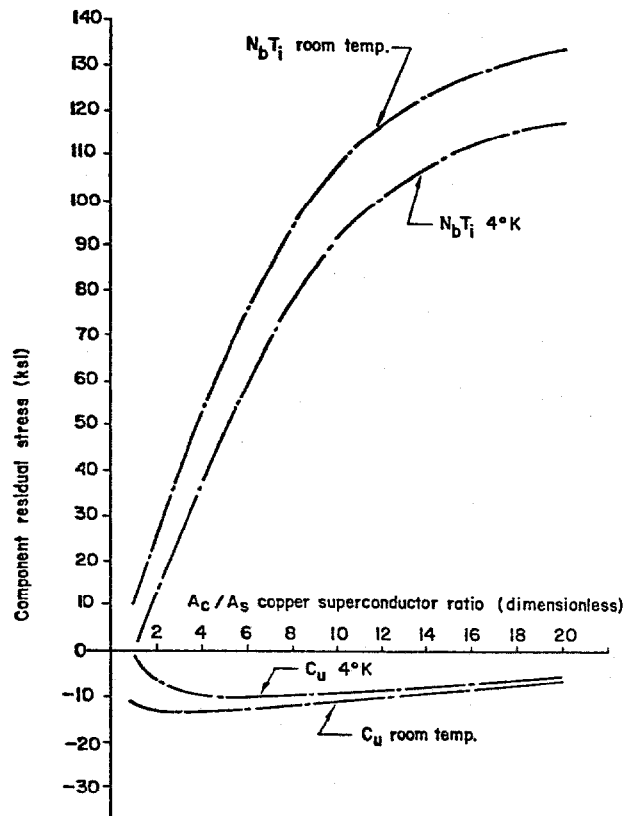


Fig. 1 Manufacturing Process
Residual Stresses

-7-

in the wire components after the manufacturing process cannot be ignored and indicates that the stress-strain interactions between the components must be studied in detail. The reader should note that figure 1 is presented as qualitative data only in that assumptions have been made as to the process used by the manufacturer. A method of measuring the residual stresses in the components will be presented later and the measured data should be used as design criteria.

3 - Twisting

To evaluate the effects of twisting an expression was developed which describes the $N_b T_i$ stress distribution across the wire cross section with respect to axial strain.

$$(5) \quad \sigma_k = E_s \left[\frac{(\epsilon + 1)^3}{(\epsilon + 1)(n^2 \pi^2 d_k^2 + 1)} \right]^{\frac{1}{2}} - E_s \left[\frac{(\epsilon + 1)^3}{n^2 \pi^2 d_k^2 + (\epsilon + 1)^3} \right]^{\frac{1}{2}}$$

where n = number of twists per inch

ϵ = wire strain (axial)

d_k = circular element mean diameter

σ_k = circular element average stress

Equation (5) was then solved using numerical methods and the specimen wire data previously shown. The results

-8-

of these calculations are presented in figure 2. The error introduced by neglecting twisting effects in earlier calculations could be corrected by applying a 6% correction factor. Since previous calculations were intended to be qualitative only the correction is not considered significant. However, for later analysis using wire test data this correction will be applied by using an effective modulus of elasticity for $N_b T_i$ of $.94 E_s$.

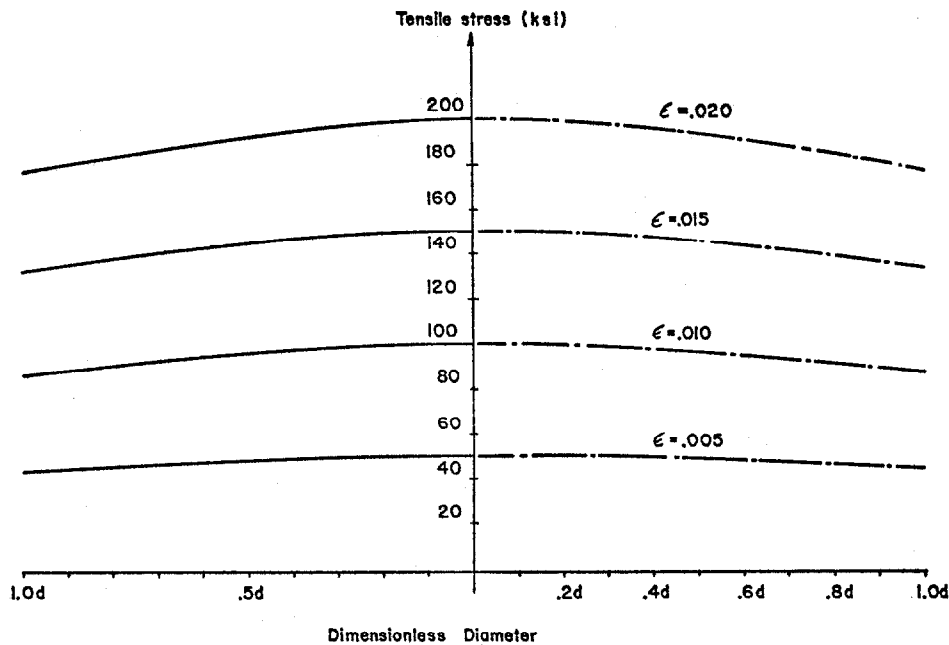


Fig. 2 $N_b T_i$ Diametral Stress Distribution

4 - Bending

Another manufacturing process which has a very important effect on superconducting coil performance is the inelastic strain introduced into the copper matrix by spooling and handling. If the wire is bent to some

-9-

radius of curvature smaller than R_{\min} the copper component will exhibit inelastic behavior at the onset of tensile loading. This effect alone will be used later to explain a superconducting coil performance characteristic described as "training". The extreme fiber strain for a circular wire wrapped onto a spool may be expressed as

$$(6) \quad \epsilon = \frac{\delta \ell}{\ell} = \frac{\pi(D + d) - \pi D}{\pi(D + d)} = \frac{d}{D + d}$$

where ϵ = extreme fiber strain

d = wire diameter

D = spool diameter

$\delta \ell$ = extreme fiber length change

ℓ = extreme fiber unstrained length

If we assume a maximum compressive prestress in the copper of 14,000 p.s.i. (see figure 1) due to previous manufacturing processes and a copper elastic limit in tension of zero (to be shown later) we can equate prestress strain to extreme fiber strain to determine R_{\min} .

Note: The following expression is simplified by assuming that the neutral axis remains coincident with the area centroid.

$$(7) \quad \frac{d}{D + d} = \frac{[\sigma_c]_{\text{prestress}}}{E_c} = \frac{14,000}{18 \times 10^6}$$

-10-

the value of E_c is taken from reference 1

Solving for D

$$(8) \quad D = 1286d$$

Equation 8 is interpreted in the following manner. If at any time during the final wire processing stages, handling, winding, etc. the wire is formed to a radius of curvature less than 643 wire diameters, the copper component will exhibit inelastic behavior only when tensile loading is applied.

Since our test specimen was delivered on a spool with a diameter much smaller than 1286d we will expect an inelastic stress-strain diagram during test.

The Bauschinger Effect

Another stress-strain interaction between wire components which may have an important effect on superconducting coil performance is the Bauschinger Effect.² If a material is loaded in tension beyond the elastic limit the elastic limit in tension is increased but the elastic limit in compression will be decreased. Similarly for compressive loading beyond the elastic limit the elastic limit in tension will be decreased. This effect will be used later to explain why poorly designed superconducting coils train to an upper limit which is lower than the design goals.

-11-

TESTS AND RESULTS

The stress-strain interactions between the superconducting wire components was studied in more detail with a straight forward tensile test. A wire specimen approximately 100 inches long was set up as shown in figure 3. Wire elongation was measured with a dial gage and the applied tensile load was measured with a spring balance. Typical load-deflection data for our specimen is presented in figure 4.

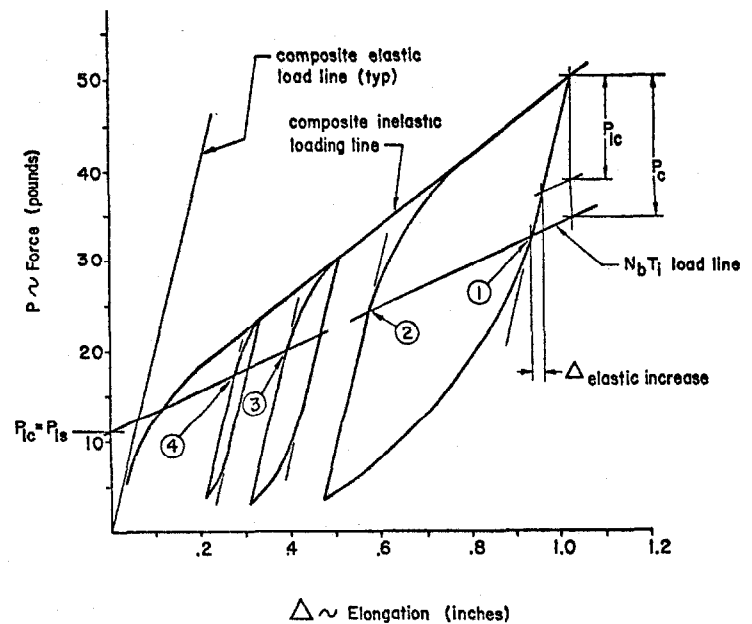
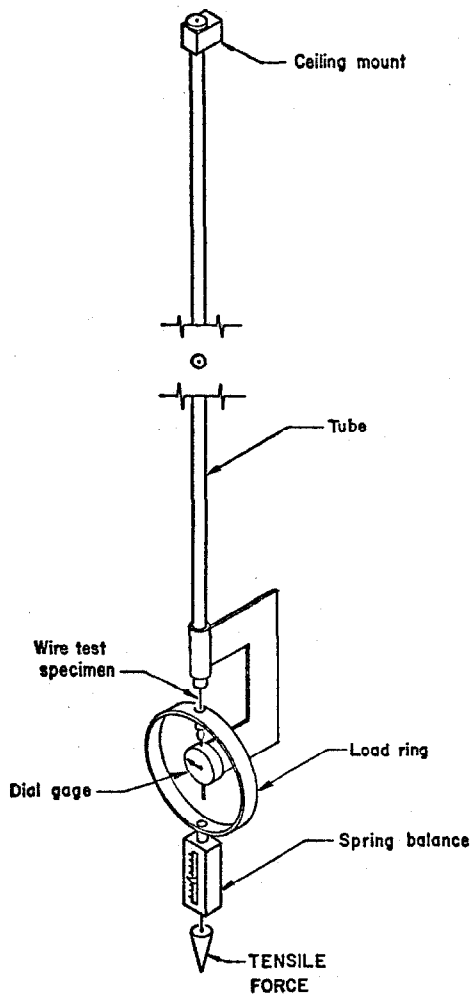


Fig. 4 Tensile Test Results

Fig. 3 Tensile Test Set Up

-12-

This data was obtained by loading the wire specimen in tension and unloading and reloading the wire to form the hysteresis loops shown. The modulus of elasticity and slope of the linear part of the composite wire load line is calculated as follows:

$$(9) \quad E_{\text{comp}} = \frac{A_C}{A_C + A_S} \left(E_C + .94 \frac{A_S}{A_C} E_S \right)$$

$$\text{Slope} = \frac{P}{\Delta} = \frac{(A_C + A_S) E_{\text{comp}}}{\ell}$$

substituting (9) into above

$$(10) \quad \text{Slope} = \frac{A_C E_C + .94 A_S E_S}{\ell}$$

where A = component cross-sectional area

.94 = twist correction factor discussed previously

ℓ = specimen original length

The slope of the loading and unloading lines were in good agreement with the slope calculated by equation (10) and they have been extended in figure 4 to show where the non-linear part of the hysteresis loop begins. A load line was also passed through the origin to show that the wire behaves inelastically at the onset of tensile loading.

The next step in evaluating the test data was to determine what part of the applied load was carried by the $N_b T_i$. Since the $N_b T_i$ behaves elastically the load line will be linear with a slope of

-13-

$$(11) \quad \text{slope} = \frac{P}{\Delta} = .94 \frac{A_s E_s}{l}$$

The location of the $N_b T_i$ load line on the wire load-deflection plot was then determined by the following method. For the large hysteresis loop shown at the right in figure 4 point 1 is the transition from elastic to inelastic behavior of the composite wire for the unloading condition. Since the $N_b T_i$ behaves elastically point 1 must be the elastic limit of the copper in compression and the force transmitted through the $N_b T_i$ component must be greater than or equal to the applied load, i.e., the $N_b T_i$ load line must pass through point 1 or above it. Similarly, point 2 corresponds to the elastic limit of the copper in tension and the $N_b T_i$ load line must pass through point 2 or below it. The $N_b T_i$ load line was then added to figure 4 and the load line passed through both points 1 and 2. The $N_b T_i$ load line also passed through points 3 and 4 which are the elastic limits of the copper in tension for the smaller hysteresis loops. It then follows that the intersection of the $N_b T_i$ load line and the vertical coordinate is the tensile loading in the $N_b T_i$ for zero applied load and this value must be equal to the compressive load in the copper prior to specimen testing. For our specimen as shown in figure 4 the pre-loading in the copper component of the wire is 11 pounds which corresponds to a compression prestress in the copper of approximately 11,000 p.s.i. The agreement between this

-14-

measured value (11,000 p.s.i.) and the calculated value (see figure 1) is considered good for the assumptions made with respect to the manufacturing process.

The three hysteresis loops in figure 4 show the Bauschinger Effect very well. Precompression of the copper due to the manufacturing process has decreased the copper tension elastic limit of our specimen to zero and the copper component of our superconducting wire has an initial elastic strain capability of

$$(12) \quad \epsilon_{\text{elastic}} = \frac{\sigma_{ic}}{E_c} = \frac{P_{ic}}{A_c E_c}$$

where subscript ic refers to initial copper and P_{ic} is the vertical intercept in figure 4.

Tensile loading and unloading of the specimen strain hardens the copper very little and the load reversal experienced by the copper shifts the tension and compression elastic limits of the copper such that Bauschinger loops are developed. The two smaller hysteresis loops show the copper compressive elastic limit to be decreasing (shifting toward the $N_b T_i$ load line) while the larger loop shows the copper elastic limit to be reduced to its limiting value of zero.

Strain hardening effects are also apparent in figure 4. For the large hysteresis loop shown in figure 4 we see that the linear part of the wire unloading line is somewhat

-15-

longer than the linear part of the smaller loops. This increase in elastic strain capability is due to strain hardening of the copper. The increase in elastic strain capability may be calculated to be

$$(13) \quad \Delta \epsilon_{\text{elastic}} = \frac{P_c + P_{ic}}{A_c E_c} \quad \text{for } |P_c| > |P_{ic}|$$

Note: for $|P_c| < |P_{ic}|$ the elastic strain capability is limited by the Bauschinger Effect to the value obtained using equation (12).

The increase in elastic elongation ($\Delta_{\text{elastic increase}}$) shown in figure 4 was then calculated to be

$$\Delta_{\text{elastic increase}} = \Delta \epsilon_{\text{elastic}} \ell = \left(\frac{P_c + P_{ic}}{A_c E_c} \right) \ell = .018$$

Figure 4 shows the elastic elongation increase measured to be in good agreement with the strain hardening predicted by equation (13).

The next test was performed to study the effects of repeated cycles to see if the area and shape of the hysteresis loop degenerated. A new piece of the same superconducting wire was set up and the small loop shown in figure 4 was repeated 15 times with no significant change in the character of the loop. The only observed change was a gradual shifting of the loop to the right. This drifting to the right is probably due to copper creep. The next test was then performed to evaluate the same size loop at higher load levels

-16-

but the same strain excursion. This test would represent a coil designed to have the same strain excursion during operation with higher wire tension used to wind the coil. The test results are presented in figure 5. The first hysteresis loop generated was the small one which corresponds to a strain excursion of less than .1%. The larger loop was then generated with a strain excursion equal to the 15 cycle excursion. The loop area was then measured and found to be approximately 28% smaller in area than the loops generated at lower load levels. This area change was to be expected since $|P_c|$ was greater than $|P_{ic}|$ and the increase in the copper elastic strain capability decreases the loop area.

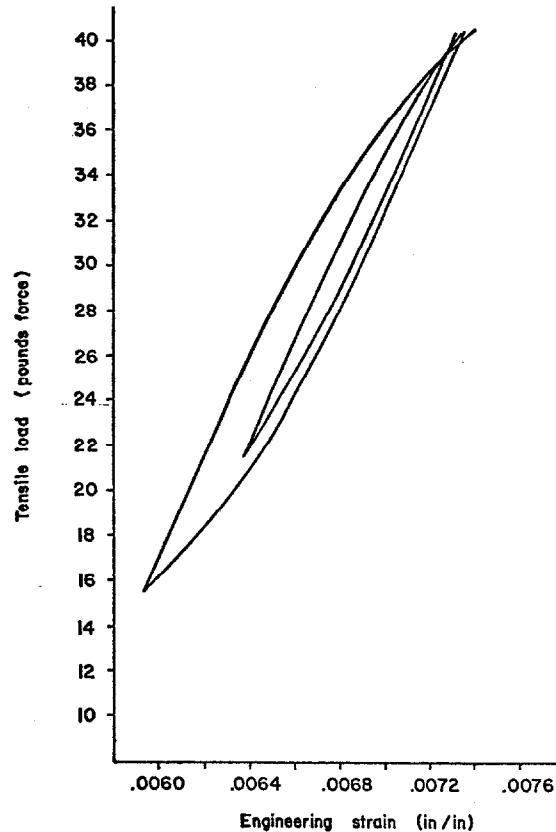


Fig. 5 Bauschinger Loops at Higher Load Levels

EVALUATION OF TEST RESULTS

To evaluate the heating potential of the above mechanical losses the thermal response of the superconducting wire is presented as a temperature rise independent of all other heating and cooling effects. Thermal calculations were simplified by assuming that the specific heat of N_bT_i is the same as copper for our temperature range and temperature-enthalpy data for copper was obtained from reference 3. The heating potential of the hysteresis loops shown in figures 4 and 5 was then calculated and the potential temperature rise (initial temperature of 4°K assumed) is shown in table 1.

TABLE 1
COIL THERMAL RESPONSE

Figure 4	heating potential (BTU/LB)	Potential Coil Temp. (°K)
Small loop	.00077	9.4°K
Intermediate loop	.0032	14°K
Large loop	.0231	23°K
Figure 5		
Small loop	.00031	7.3°K
Large loop	.00118	16.2°K

Further discussion as to the effect of mechanical losses on a specific coil design will not be discussed here since detailed coil analysis is beyond the scope of this paper. However, sample calculations for a superconducting solenoid coil constructed with our wire specimen showed mechanical losses to

be several times greater than electrical losses.

The next interpretation of our test results is a description of coil training which is due to inelastic behavior of the copper. The following description is considered qualitative only, i.e., a quantitative analysis must account for all heating and cooling peculiar to a specific coil design and operating system. Point 1 in figure 6 represents the initial condition of our wire specimen prior to charging the coil for the first time. When the coil is energized for the first time the copper experiences plastic deformation at the onset of tensile loading and proceeds to point 2 where the coil quenches. The wire then unloads along line 2-3 (slope given by equation 10) to point 3. When the coil is energized a second time the wire reloads along line 3-2 and then proceeds to point 4 where the coil quenches again. In this manner the coil continues to train to higher levels but the training gain becomes progressively smaller. The strain excursion eventually exceeds the initial elastic strain capability of the copper (equation 12)

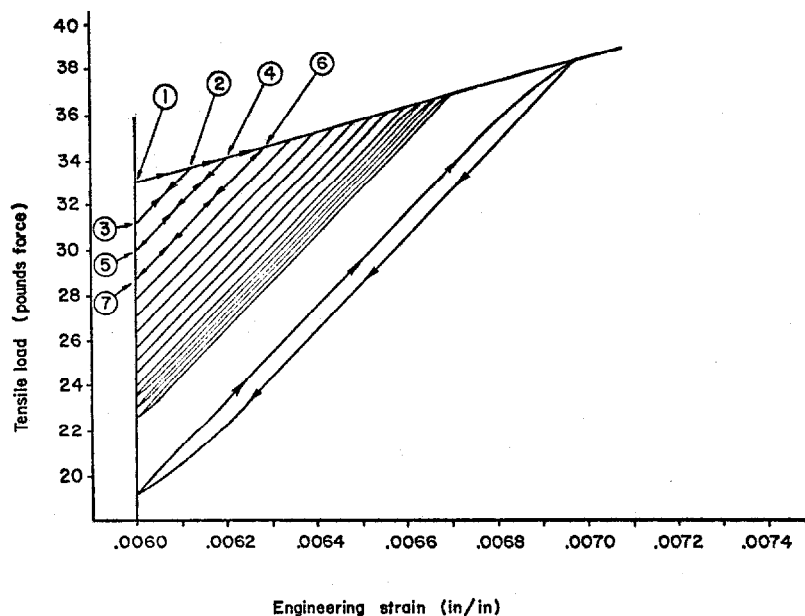


Fig. 6 Graphical Description of Training

and Bauschinger loops begin to develop. Finally, after many quenches the coil trains to its design value. The hysteresis loop shown in figure 6 represents the final Bauschinger loop for a coil designed to operate with a maximum strain excursion (hoop strain) of approximately .001 (see reference 4). For this example the coil has trained satisfactorily to full field, however, the coil performance may not be satisfactory if the charge time period is limited. Approximately half of the heat generated by the hysteresis loop is generated during the final 15% of the strain excursion at the end of the charge transient and this rate of heat generation may limit the charge time to longer periods than the design value. Finally, for poorly designed coils (see reference 4) severe Bauschinger loops may develop at currents and fields well below the design goals such that the coil will never reach its design values.

COIL DESIGN CONSIDERATIONS

- 1 - If forces are applied to a real material the material will experience deformations. Even if the boundaries of the coil (reaction members) approach infinite rigidity, the current conductors will still experience deformations when the coil is energized due to a redistribution of forces within the coil structure. One should not be misled into believing that prestressing will eliminate conductor motion. Prestressing may be used to limit conductor motion only.
- 2 - If prestressing is used to limit conductor motion, loss of preload due to relaxation of the coil and structure during construction and differential contractions due to cool down

- should be evaluated.
- 3 - The elastic limits of the matrix metal used to stabilize the superconductor may be much lower than the yield strength. Stress analyses using standard engineering practice can result in a coil which is sound structurally but unsatisfactory thermally. Stress analysis only does not contribute to an understanding of coil stability. A detailed deflection analysis must be done and the heat generated by inelastic deformations must be accounted for if thermal stability is to be guaranteed.
 - 4 - The stress-strain interactions between the metallic partners which make up the conductor composite must be studied in detail. A thorough understanding of these interactions identifies mechanical losses which have been neglected and establishes new "ground rules" for the development of coil designs which are mechanically stable.
 - 5 - Coil parameter studies must be conducted which show the "trade-off" of all magnet thermal, structural, electrical and fluid flow parameters if optimum design is to be achieved. For example, sample calculations using the mechanical loss data presented herein show that the electrical losses in the copper are much lower than the mechanical losses for most coil designs. Therefore some cold working of the copper to increase its elastic strain capability should greatly improve coil performance and decrease the size of the reaction members, i.e., soft copper is not the best choice for an optimum design.
 - 6 - The mechanical losses described herein may be eliminated by careful design and construction. The Bauschinger Effects

may be eliminated completely by strain hardening the copper a modest amount to increase its elastic strain capability. The coil designer can then measure the elastic strain capability of the finished wire to verify that the maximum strain experienced by the wire during coil operation is less than the measured value. The coil builder can also eliminate the inelastic copper losses associated with training by improving the stress distribution in the copper. The following discussion describes a method of accomplishing same after the coil is wound.

THE PWP PROCESS

The PWP process (post wind preload) has been invented⁵ to change the stress distribution in the copper component of superconducting wire so that the copper will behave elastically during coil operation. After the coil has been completely wound a system of forces is applied to the coil and the strain experienced by the copper changes the stress distribution in the copper. In simple terms we might describe the process effect as a history eraser. The undesirable effects of spooling, handling, etc. are eliminated by prestressing the copper to a level greater than the operational stress. Figure 7 shows one method of performing the PWP process. The coil (solenoid shown) is wound on a mandrel made from a material which has a very low coefficient of expansion (invar or equivalent). After the coil is completely wound and cured (potted construction assumed) the coil with mandrel is cooled to 77°K with liquid nitrogen. Due to the contraction differential between copper and mandrel the copper component of the coil turns adjacent to the

bore will experience hoop strains approaching .3%. The coil is then warmed to room temperature and the mandrel is removed which completes the process.

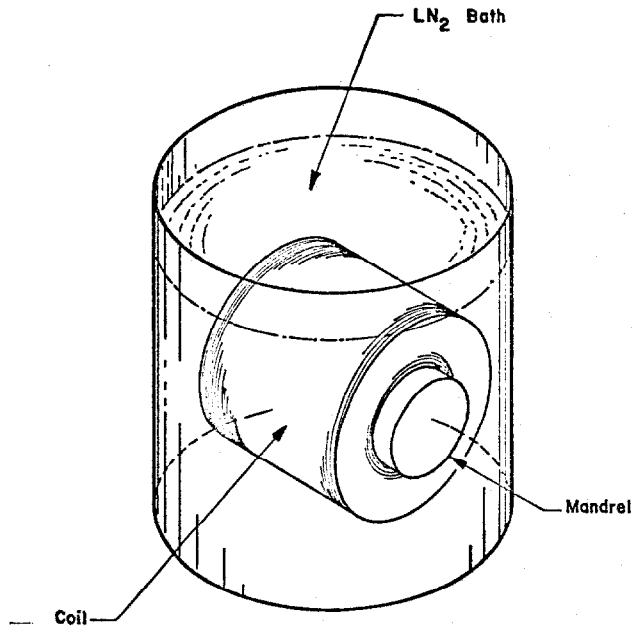


Fig. 7 The PWP Process

CONCLUSIONS AND FUTURE WORK

Inelastic behavior of the matrix metal used to stabilize superconductors should be treated as a mechanical loss which generates heat. These mechanical losses can be identified by material testing and eliminated with good design, careful construction and post wind preloading.

Electrical losses which generate heat during the charge and discharge transients may not be as great as previously measured⁶ if mechanical losses were also present when electrical loss measurements were made. Future test coils designed to operate without mechanical losses should confirm this statement.

As soon as possible a superconducting solenoid test coil will be designed and built to verify that the above mechanical losses may be eliminated. The superconducting wire used to wind the test coil will be tensile tested at both room temperature and low temperatures. The coil performance test data will then be correlated with wire test results and detailed structure calculations to develop better coil design criteria.

Acknowledgements

The author wishes to acknowledge J. Jagger for his assistance in preparing the figures and H. Hart who helped with wire testing.

REFERENCES

- 1 Schwartzberg, F. R., et al, Cryogenic Materials Data Handbook, AD609562 (Martin Company, Denver, Colorado) latest revision August 1968, page F.1.ij
- 2 Timoshenko, S., Strength of Materials, Part II, Advanced Theory & Problems, Third Edition, pages 412-417
- 3 Properties of Materials at Low Temperatures, Phase I, Cryogenic Engineering Laboratory, Boulder, Colorado, page 4.112-1
- 4 Westendorp, W. F. & Kilb, R. W., Stresses in Magnetic Field Coils, Proceedings of the 1968 Summer Study on Superconducting Devices and Accelerators, Part III, page 723, figure 3, Radial Motion, page 726, figure 8
- 5 Record of Invention filed May 14, 1974, AEC Case number S-44, 379
- 6 W. B. Sampson, et al, Superconducting Synchrotron Magnets, Particle Accelerators, 1970, Vol. 1, page 173-185